Available online at
http://uppp.uitm.edu.my/online-issues.html

e-ISSN: 2689-4934

ESTEEM Academic Journal Vol 20, September 2024, 168-182

ESTEEM
Academic Journal
(EAJ)

# Optimization of methylene blue dye degradation using heterogeneous Fenton-like reaction with $Fe_3O_4$ nanoparticles/PVDF macrospheres: A response surface methodology approach

Mohamed Syazwan Osman[1*,2,3], Huzairy Hassan[2], Sung-Ting Sam[2,3], Nadzirah Balqis Mohd Nazeri[1], Mohd Syafiq Abdul Wahab[4], Rasyidah Alrozi[1], Hafawati Rosdi[1], Maya Fitriyanti[5]

[1]*EMZI-UiTM Nanoparticles Colloids & Interface Industrial Research Laboratory (NANO-CORE), Chemical Engineering Studies, College of Engineering, Universiti Teknologi MARA, Cawangan Pulau Pinang, 13500 Permatang Pauh, Pulau Pinang, Malaysia.*
[2]*Faculty of Chemical Engineering & Technology, Universiti Malaysia Perlis, 02600 Arau, Perlis, Malaysia.*
[3]*Center of Excellence Geopolymer & Green Technology (CEGeoTech), Universiti Malaysia Perlis (UniMAP), 01000 Kangar, Perlis, Malaysia.*
[4]*EMZI Holding Sdn Bhd, 1st Floor, SP Plaza Tower, Jalan Ibrahim, 08000 Sungai Petani, Kedah, Malaysia*
[5]*School of Life Sciences and Technology, Institut Teknologi Bandung, Bandung 40132, Indonesia.*

ARTICLE INFO

*Article history:*
Received 30 June 2024
Revised 18 August 2024
Accepted 26 August 2024
Online first
Published 30 September 2024

*Keywords:*
Methylene blue dye
Iron oxide nanoparticles
PVDF
Macrospheres
Optimization
Response surface methodology

ABSTRACT

A heterogeneous Fenton-like reaction was investigated in this study using $Fe_3O_4$ nanoparticles/polyvinylidene fluoride macrospheres for the degradation of methylene blue (MB). MB dye is one of the most common contaminants found in industrial wastewater, and its degradation is considered critical from both an environmental and public health perspectives. In this work, using Response Surface Methodology coupled with the Box-Behnken Design, a systematic investigation on the effects of the initial pH, catalyst loading, and $H_2O_2$ dosage on degradation efficiency was performed. The obtained optimal conditions were pH 7, catalyst loading of 10 g/L, and dosage of $H_2O_2$ at 10 mM, which resulted a maximum degradation efficiency of 99.94%. The results showed that the efficiency of the Fenton-like reaction was obviously favoured by neutral pH, making a good balance between hydroxyl radical generation and catalyst stability. According to the ANOVA results, initial pH, catalyst loading, and $H_2O_2$ dosage are

[1*] Corresponding author. *E-mail address*: syazwan.osman@uitm.edu.my
https://doi.org/ 10.24191/esteem.v20iSeptember.1860.g1828

*DOI:* 10.24191/esteem.v20iSeptember.1860.g1828

significant factors, and among those three, pH is the most critical one. Validation experiments demonstrated the predictive accuracy of the model, showing small percentage errors between experimental and predicted values.

## 1. INTRODUCTION

The presence of organic dyes in wastewater is complex and has significant implications for achieving the Sustainable Development Goals (SDGs) [1]. This issue is intricately linked to SDG 6 (Clean Water and Sanitation) because the release of these pigments degrades water quality, exacerbates pollution, and affects the accessibility of freshwater resources [2]. It is essential to address the environmental impacts of organic dyes to promote environmental sustainability, protect human health, and attain economic success, as outlined in the 2030 Agenda for Sustainable Development.

Methylene Blue (MB) is a cationic dye with extensive use in the textile, printing, and pharmaceutical industries due to its striking color and persistence [3]. However, the broad utilization of this chemical originates concerns regarding its potential health and ecological impact. MB is considered to be carcinogenic and mutagenic, hence, it leads to doubts about human beings exposed to it [4]. It has been observed that long-term exposure to MB through ingestion, inhalation, or skin contact causes hazardous health issues such as skin irritation, respiratory disorders, and potentially carcinogenic properties [5]. Regulatory agencies have thus imposed strict limits on the levels of MB in consumer products and at the wastewater discharge level to ensure public health safety [6]. There is thus a strong need for effective treatment methods for wastewater and stringent regulations to reduce the environmental impacts of MB contamination. Several physical, chemical, and biological methods have been investigated to solve the problem of MB dye pollution in wastewater.

Physical methods involve the removal or separation of MB from water by adsorption onto activated charcoal or by membrane filtration [7-8]. Chemical methods involve the chemical degradation of MB into less harmful products; AOPs have proven very effective in degrading organic pollutants like MB [9]. The generated •OH radicals are highly reactive in AOPs, thus decomposing MB molecules into smaller, less toxic species. Fenton and Fenton-like reactions are among the most common chemical methods studied for the degradation of MB, as they generate •OH radicals under mild conditions [10].

Employing iron-based catalysts, such as ferrous sulphate ($FeSO_4$), these reactions decompose $H_2O_2$ to produce •OH radicals [11]. Chemical methods have promising potential for tackling MB dye pollution and thus find their application on a broad scale in wastewater treatment. Iron oxide nanoparticles, particularly $Fe_3O_4$ nanoparticles, have demonstrated potential as catalysts for heterogeneous Fenton-like reactions in wastewater treatment [12].

These nanoparticles exhibit excellent catalytic properties, which allow the formation of •OH radicals, an essential step in Fenton-like reactions [13]. However, one of the major challenges is that they tend to aggregate, which reduces their catalytic activity and colloidal stability in aqueous media [14]. Aggregation is due to electrostatic interactions, van der Waals forces, as well as surface chemistry [15-16]. The application of polymer matrices to stabilize the nanoparticles and avoid their agglomeration has also been investigated by scientists. Entrapment of iron oxide nanoparticles into polymeric matrices, more exactly poly-vinylidene fluoride PVDF macrospheres, will immobilize the nanoparticles for enhancing their reusability in wastewater treatment due to additional durability [17-18].

This novel technique enhances catalysis efficiency, and the ease of retrieval and reuse, thus promoting sustainable and eco-friendly approaches towards wastewater treatment [19]. The incorporation of nanoparticles into a polymeric matrix has two advantages: it enhances synergistic interactions and diminishes the release of nanoparticles into treated water [20]. This technique is suitable for large-scale engineering applications and offers a flexible and cost-effective solution to water pollution.

Although $Fe_3O_4$ nanoparticle/PVDF macrospheres have the ability to degrade pollutants through heterogeneous Fenton-like reactions, there is a lack of information in the literature regarding the optimization of reaction conditions. The degradation efficiency is greatly influenced by the catalyst dose, pH, and concentration of $H_2O_2$. However, the optimal values for these factors have not yet been identified [21]. Response Surface Methodology (RSM) in conjunction with Box –Behnken design (BBD) effectively overcomes this deficiency by methodically optimizing the reaction parameters [22]. RSM facilitates a systematic examination of response surfaces, which allows the identification of nonlinear relationships between variables and responses. It also helps establish ideal conditions with the least number of experiments [23]. The Box-Behnken design improves the efficiency of experiments by examining the response surfaces with a restricted number of trials, thereby enabling the development of a second-order polynomial model for predicting answers [24].

The main aim of the present study was the use of Response Surface Methodology and Box-Behnken design in order to maximize the breakdown of Methylene Blue dye, employing $Fe_3O_4$ nanoparticles/PVDF macrospheres through a Fenton-like reaction. This work will serve to highlight the most optimal conditions for pollutant removal by means of precise manipulation of catalyst dosage, pH, and $H_2O_2$ concentration. The RSM method is outstanding for the development of complex systems with multiple variables and for reducing the number of necessary experiments [25-26]. The use of Response Surface Methodology (RSM) and the Box-Behnken design (BBD) enabled the methodological optimization of reaction conditions through a comprehensive investigation of the parameters that influence the efficiency of MB deterioration.

## 2. MATERIALS & METHODS

### 2.1 Materials

All the chemicals and reagents used in this study were of analytical grade and used directly without further purification. $FeCl_3 \cdot 6H_2O$ (97% purity, ACS reagent grade) and ammonium hydroxide solution (28% $NH_3$ in $H_2O$) were obtained from Sigma Aldrich. The compound that is derived from QRëC was Iron(II) sulfate heptahydrate ($FeSO_4 \cdot 7H_2O$), purity of 99.5% (analytical reagent grade). A 35% pure (chemically pure grade) hydrogen peroxide ($H_2O_2$) was obtained from R & M Chemicals. Denatured absolute ethanol ($C_2H_5OH$) with 99.7% purity was acquired from Fine Chemicals. Sigma Aldrich supplied Poly (vinylidene fluoride) (PVDF) with a molecular weight of ~ 534,000. Meanwhile, Fisher Scientific (M) Sdn Bhd provided the Dimethyl sulfoxide (DMSO) solvent. The sodium dodecyl sulphate (SDS) used in this study was obtained from Merck, Germany, and was approximately 95% pure, as determined by the total alkyl sulfate concentration. The MB dye (Sigma) was of analytical grade. The studies utilized Milli-Q deionized water with a resistivity of 18 MΩ·cm obtained from a potable water source. Water was collected using a PureLab Option-Q system.

### 2.2 Synthesis of $Fe_3O_4$ nanoparticles

$Fe_3O_4$ nanoparticles were produced using a widely accepted coprecipitation technique in a controlled environment [27]. The experimental procedure consisted of creating an oil bath by adding 1 kg of palm oil to a stainless-steel bowl. Afterwards, a nitrogen gas pipeline was attached to a 250 mL three-neck flask that held approximately 70% (175 mL) of deionized water. Next, $FeSO_4 \cdot 7H_2O$ (2.7802 g) and $FeCl_3 \cdot 6H_2O$ (5.8115 g) were dissolved in deionized water in a flask. This resulted in a molar ratio of 1:2 between $FeSO_4 \cdot 7H_2O$ (0.01 moles) and $FeCl_3 \cdot 6H_2O$ (0.02 moles). The solution was vigorously blended while heated to 80 °C with constant stirring under a continuous flow of $N_2$ gas. Once the desired temperature was reached, the rapid addition of 20 mL $NH_4OH$ solution caused a noticeable colour change from brown to completely

https://doi.org/ 10.24191/esteem.v20iSeptember.1860.g1828

black. The solution was then vigorously agitated for an additional 10 min, after which the flow of $N_2$ gas was stopped and the solution was naturally cooled to room temperature. The formed black precipitate of $Fe_3O_4$ nanoparticles was separated by centrifugation at a speed of 2700 rpm for 10 min. Then, the solid particles were washed throughly with 20 mL of ethanol and 20 mL of deionized water until the pH dropped from 9 to 6, thus removing any residual ionic impurities. At last, the $Fe_3O_4$ nanoparticles were dispersed in deionized water for future use and investigation.

For the preparation of the PVDF solution, 10 g of PVDF powder was dried in a vacuum oven at 25 °C for 5 h. After this process, dehydrated PVDF powder was dissolved in 90 g of DMSO in a beaker. A sensor tip of a thermometer was inserted into the solution to monitor any fluctuation in the temperature. Following the addition of the PVDF powder, the mixture was immediately sealed with Parafilm and constantly stirred at 250 rpm. The mixture was then heated from ambient temperature to 60 °C at 10 °C/min and then held for 60 min at this temperature with constant heating to ensure the formation of a homogeneous solution. Afterwards, the solution was cooled to 40 °C andleft undisturbed overnight while continuously stirring at 150 rpm. This was taken to minimize the formation of trapped air bubbles.

The $Fe_3O_4$ nanoparticle/PVDF solution was obtained by adding 0.15 g of synthesised $Fe_3O_4$ nanoparticles into 30 g of the PVDF polymer solution. The addition was done in a particular order to ensure the best dispersion. First, all the $Fe_3O_4$ nanoparticles were uniformly distributed in a 10 g PVDF solution in a 20 mL glass vial by highly energetic sonication for at least 20 min to ensure total dispersion. The homogeneous nanoparticle-PVDF solution was then gradually incorporated into the remaining PVDF solution under the application of sonication for another 30 min. Successive processes were quintessential for ensuring proper distribution of the nanoparticles within the polymeric solution, thereby maintaining future experimental procedures' consistency and reliability.

$Fe_3O_4$ nanoparticle/PVDF macrospheres were fabricated by using the phase inversion method. Firstly, $Fe_3O_4$ nanoparticle/PVDF solution was sonicated for 10 min. Then it was extruded from a syringe needle, size 27G (with diameter of 0.4 mm) at controlled pumping speed about 1.0 mL/min by a Peristaltic Pump (KFS series, Kamoer, China). To induce macrosphere development, the polymer solution was gradually and slowly added to droplets in the coagulation bath prepared by dissolving 0.5 wt. % of sodium dodecyl sulphate (SDS) in deionised (DI) water. Since it is often observed that the microcapsules tend to build up or cluster in one particular region, the coagulation bath was manipulated manually. The macrospheres were left in a coagulation bath overnight to ensure total solidification and remove the residual solvent. The macrospheres were then collected from the coagulation wash and stored in a desiccator for further analysis.

### 2.3 Degradation of methylene blue dye (MB) procedures

Methylene blue was used as the representative dye pollutant for evaluating the catalytic performance of $Fe_3O_4$ Nanoparticles/PVDF Macrospheres. MB degradation was investigated by the Fenton-like method. Further tests were conducted to ensure that the results were reliable and consistent. Each trial consisted of glass vials containing 15 mL of solution with an initial dye concentration of 100 ppm. Subsequently, 5 mL of hydrogen peroxide was added to the solution and stirred at 30 rpm in order to ensure through mixing. The batch experiments were carried out by adding the $Fe_3O_4$ nanoparticle/PVDF macrospheres to a solution and swirling it at a speed of 80 rpm. All experiments commenced right after adding the nanoparticles at room temperature conditions. Stirring was assisted with the use of a SCILOGEX Analogue Tube Rotator, USA. The dosage of $Fe_3O_4$ nanoparticle/PVDF macrospheres varied within the range of 5 to 15 g/L, whereas the amount of hydrogen peroxide was in the range of 10-30 mM. The experimental temperature was approximately 30 °C. The pH was initially adjusted in the range of 3 to 7.

After the reaction, the separation of $Fe_3O_4$ nanoparticles/PVDF macrospheres was done using a neodymium boron ferrite cylindrical magnet from outside, with its surface magnetization approximately equal to 6000G (Ningbo YuXiang E&M Int'1 Co., Ltd.). Spectrophotometric analysis was conducted on a UV-Vis C-7200UV instrument (China). The absorbance was read at a maximum wavelength of 664 nm,

https://doi.org/ 10.24191/esteem.v20iSeptember.1860.g1828

both initially and after 3 h of testing. The measurements were then compared with a preexisting standard calibration curve to calculate the concentration of MB. After that, 0.2 mL of the reaction solution was extracted and then analyzed by UV−vis spectroscopy.

### 2.4 Box-Behnken design

Response Surface Methodology (RSM) is a useful approach for optimizing the interaction of different parameters to obtain the best results. One significant benefit in this context is the utilization of the Box-Behnken design (BBD) [28]. This design process is particularly advantageous when working with incomplete factorial designs with four levels. BBD utilizes mathematical models that incorporate the coefficients of both the first and second degrees. A quadratic model forms the basis for estimatingparameters by developing a relationship between the experimental factors and the observed results. The relationship is empirical and of the second-order variety [29].

For instance, consider an objective that aims at the optimization of MB decolorization effectiveness, which would be centered on three factors: the amount of catalyst used, initial pH, and $H_2O_2$ concentration. This approach was followed by trials for each of these elements at three different levels: -1, 0, and +1. The RSM allows the researcher to efficiently search the problem space and, hence, provides valuable insights into the development of optimal solutions tailored to specific conditions [30].

## 3. RESULTS AND DISCUSSION

### 3.1 Dye degradation and model fitting

In this work, RSM was applied to investigate the optimization of the relationship between many independent variables and the values of some important parameters by BBD. The experimental data was checked for correctness and efficiency using the Design-Expert program, version 13. This methodology is widely applied in the investigation of a wide range of processes, such as the discoloration of MB. All the experiments in our study were designed based on Response Surface Methodology, RSM, which effectively reduces the cost and time needed for the processes.

We studied the effects of three major factors, initial pH (A), catalysts (B), and $H_2O_2$ dosage (C), on MB degradation. In total, seventeen trials were conducted in duplicate to assist in the statistical modeling of the studies. The independent variables were assessed at two levels: low (-1) and high (+1). Table 1 illustrates the experimental ranges of independent variables.

Table 1. Experimental Design Using the Box−Behnken Method: Variable Settings and Levels

| **Variables** | **Units** | **Range of levels** | | |
|---|---|---|---|---|
| | | **-1 (minimum)** | **0 (median)** | **+1 (maximum)** |
| Initial pH (A) | | 3 | 5 | 7 |
| Catalyst loading (B) | g/L | 5 | 10 | 15 |
| $H_2O_2$ dosage (C) | mM | 10 | 20 | 30 |

Response Surface Methodology (RSM) was used to statistically analyze the processes, explore their interactions, and optimize the procedures. The Box-Behnken design (BBD) model evaluates three independent variables, and their responses are summarized in Table 2. The results revealed significant variability in the ((MB) decolorization efficiency under different experimental conditions. The highest decolorization efficiency of 99.77% was achieved at an initial pH of 7, a catalyst loading of 10 g/L, and an $H_2O_2$ dosage of 10 mM (Run 4). This indicated that a neutral pH significantly enhanced the efficiency of the Fenton-like reaction. At pH 7, the generation of hydroxyl radicals, which are the primary reactive species in the Fenton-like reaction, was maximized.

https://doi.org/ 10.24191/esteem.v20iSeptember.1860.g1828

Additionally, the $Fe_3O_4$ catalyst remained stable within the PVDF porous macrospheres, reducing the likelihood of iron leaching, which is a significant issue under acidic conditions [18]. The stability of the $Fe_3O_4$ nanoparticles at this pH ensures consistent catalytic activity, facilitating a more efficient degradation process [31]. Furthermore, a neutral pH balances $H_2O_2$ availability and hydroxyl radical generation, optimizing the reaction for maximum dye degradation [32].

Conversely, the lowest efficiency of 92.68% occurred at an initial pH of 3, a catalyst loading of 5 g/L, and $H_2O_2$ dosage of 20 mM (Run 15). Acidic conditions likely do not favor degradation. At lower pH levels, excessive hydroxyl radical generation can lead to rapid consumption, decreasinge availability for MB degradation [33]. Moreover, acidic conditions can enhance iron leaching from $Fe_3O_4$ nanoparticles, thereby reducing their catalytic activity and stability [34]. The lower catalyst loading further exacerbates the inefficiency due to to fewer active sites, and a higher $H_2O_2$ dosage causes a scavenging effect, decreasing the overall degradation efficiency [33].

Runs at the central point (pH 5, catalyst loading of 10 g/L, and $H_2O_2$ dosage of 20 mM) consistently resulted in approximately 94.05% decolorization efficiency. Although these conditions provide stable results, they are not optimal for achieving the highest degradation efficiency. The central point conditions suggest that a moderate pH and catalyst loading can maintain a steady reaction environment; however, the balance is insufficient to maximize hydroxyl radical generation and utilization. The median $H_2O_2$ dosage, although providing reasonable oxidative power, still risks the scavenging effect if it is not perfectly balanced with radical generation. Fine-tuning each parameter is essential to achieve maximum dye degradation efficiency.

Based on the data in Table 2, it can be inferred that the quadratic model is the most suitable mathematical model. Therefore, the final equation that considers the coded factors is given by Eq. (1) follows:

$$\text{MB decolorization} = 94.0498 + 2.15992A + 0.845081B + -0.779487C + -0.731461AB + -0.124208AC + 0.0776785BC + 1.8173A^2 + 0.810416B^2 + 0.93714C^2 \quad (1)$$

A, B, and C correspond to the initial pH, catalyst loading, and $H_2O_2$ dosage, respectively. Equations built using the encoded factors can be utilized to make predictions about the behavior of a particular level of each factor. The factors are typically assigned a code of +1 for higher values and -1 for lower values. The encoded equation can also be used to evaluate the relative importance of variables by comparing the factor coefficients.

The equation demonstrates that the positive coefficient for the initial pH value (2.15992) emphasizes the substantial influence of pH on the effectiveness of degradation. This indicates that a pH value of 7, which is considered neutral, offers ideal conditions for this process. The efficiency was positively influenced by the catalyst loading (0.845081), but to a lesser degree. This suggests that higher quantities of $Fe_3O_4$ nanoparticle/PVDF macrospheres improve the degradation process until they reach an optimal value. On the other hand, the negative coefficient for $H_2O_2$ dose (-0.779487) indicates that increasing the amount of $H_2O_2$ may decrease the efficiency. This is likely because the excess $H_2O_2$ consumes hydroxyl radicals without contributing to dye degradation, which is known as the scavenging effect.

The interaction terms AB (-0.731461) and AC (-0.124208) suggest that the combined changes in these parameters result in a modest decrease in efficiency. The presence of optimal ranges for each factor is indicated by the positive quadratic terms ($A^2$, $B^2$, and $C^2$), with the quadratic influence of starting pH (1.8173) being the most important.

https://doi.org/ 10.24191/esteem.v20iSeptember.1860.g1828

Table 2. Actual Experimental Results Obtained through a Box−Behnken Design

| Run | Factor A<br>A:initial pH | Factor B<br>B:Catalyst loading<br>mg/L | Factor C<br>C:$H_2O_2$ dosage<br>mM | Experimental response<br>MB decolorization<br>% |
|---|---|---|---|---|
| 1 | 1 | 0 | 1 | 98.25 |
| 2 | 0 | 0 | 0 | 94.05 |
| 3 | 0 | -1 | 1 | 94.26 |
| 4 | 1 | 0 | -1 | 99.77 |
| 5 | 0 | 0 | 0 | 94.05 |
| 6 | -1 | 1 | 0 | 96.45 |
| 7 | 1 | 1 | 0 | 99.21 |
| 8 | 0 | 0 | 0 | 94.05 |
| 9 | 1 | -1 | 0 | 98.37 |
| 10 | -1 | 0 | 1 | 94.09 |
| 11 | 0 | 1 | 1 | 95.49 |
| 12 | -1 | 0 | -1 | 95.11 |
| 13 | 0 | 0 | 0 | 94.05 |
| 14 | 0 | -1 | -1 | 96.26 |
| 15 | -1 | -1 | 0 | 92.68 |
| 16 | 0 | 0 | 0 | 94.05 |
| 17 | 0 | 1 | -1 | 97.18 |

## 3.2 Analysis of variances (ANOVA) and regression analysis

Response Surface Methodology (RSM) was employed to optimize the examination of the relationship between various independent variables and the values of important parameters using the Box-Behnken design (BBD). The experimental data was evaluated for correctness and efficacy using the Design-Expert program (version 13). The importance of the quadratic model was confirmed by analysis of variance (ANOVA) [22]. Table 3 demonstrates the variables that affect the effectiveness of methylene blue (MB) degradation through a heterogeneous Fenton-like reaction using $Fe_3O_4$ nanoparticles/PVDF macrospheres. The model's robudtness is demonstrated by an F-value of 60.14 and a p-value of less than 0.0001.

The initial pH had the highest impact, as indicated by a sum of squares value of 37.32, an F-value of 278.76, and a p-value of less than 0.0001, highlighting its critical involvement in Fenton-like reactions. A neutral pH of 7 ensures the optimal production and stability of hydroxyl radicals, thereby maximizing degradation efficiency. According to the literature, it is commonly observed that the ideal pH for this phenomenon is typically falls within the range of neutral to slightly acidic, as reported in reference [31]. Within this specific pH range, the generation of hydroxyl radicals is optimised, and the catalytic efficiency of the $Fe_3O_4$ nanoparticles reaches its highest point, resulting in the most efficient decomposition of methylene blue. Conversely, if the pH is too low, it can result in the excessive dissolution of iron, leading in side reactions and a decrease in catalytic effectiveness [18], [34]. The relevance of pH is related to its influence on the formation of hydroxyl radicals, which are crucial for the degradation process [33].

The deterioration is considerably influenced by the catalyst loading, as indicated by a sum of squares value of 5.71, an F-value of 42.67, and a p-value of 0.0003. Optimal catalyst loading ensures an ample number of active sites for reactions. Nevertheless, the presence of the quadratic term ($B^2$) suggests a

https://doi.org/ 10.24191/esteem.v20iSeptember.1860.g1828

nonlinear impact, whereby an excessive amount of catalyst leads to the aggregation of nanoparticles, resulting in a decrease in surface area and catalytic efficiency [35]. Excessive loading might result in mass transfer limits, which in turn reduces efficiency [36].

The dosage of hydrogen peroxide impact deterioration, as indicated by a sum of squares value of 4.86, an F-value of 36.31, and a p-value of 0.0005. The optimal concentration of $H_2O_2$ is crucial because it acts as a source of hydroxyl radicals. The presence of the quadratic term ($C^2$) indicates that an excessive amount of $H_2O_2$ can lead to scavenging effects, which in turn reduce the availability of hydroxyl radicals for degradation [31]. This phenomenon of scavenging has been recorded in the literature.

The correlation between the initial pH and catalyst loading (AB) was statistically significant (F-value 15.98, $p = 0.0052$), suggesting that both parameters should be optimized to achieve the best degradation results. However, the lack of significant interactions between pH and $H_2O_2$ dosage (AC) and between catalyst loading and $H_2O_2$ dosage (BC) indicates that the relationship between these factors does not have a major impact on the degradation of MB within the range of the study. The BC interaction may be attributed to the saturation of the catalyst sites. When the catalyst loading is increased, there is a sufficient number of active sites on the $Fe_3O_4$ nanoparticles to effectively use the $H_2O_2$ that is present. When the amount of $H_2O_2$ is increased beyond a specific threshold, it has no major impact on the reaction because the catalyst is already fully saturated. In the case of AC contact, it has been previously stated that the reaction is pH-dependent, meaning that the initial pH level is a crucial component that affects the effectiveness of the Fenton-like reaction. If the reaction is carried out at an optimum pH, variations in the $H_2O_2$ dosage may not have a significant influence because pH dictates the efficiency of hydroxyl radical generation.

The residual sum of squares is 0.9372, and the mean square of the residual is 0.1339, suggesting that the model fits well with the experimental data. The lack-of-fit test, with a p-value greater than 0.05, verifies the model's adequacy and the random distribution of residuals, thus verifying the model's predictive power [37]. These data highlight the significance of optimizing the starting pH, catalyst loading, and $H_2O_2$ dosage to achieve the effective degradation of MB. The observed influence of the starting pH is consistent with prior research on ideal Fenton reactions, which often occur at pH levels ranging from slightly acidic to neutral [34]. The beneficial impact of increasing the catalyst loading until aggregation underscores the necessity for meticulous optimization [38]. With the exception of AB, the limited importance of interaction terms streamlines the optimization process by prioritizing the most relevant parameters, thereby easing practical implementations.

Following is the result of the regression analysis of the ANOVA, represented in Table 4, which affords deeper insight into model accuracy and predictive ability concerning the description of MB degradation effectiveness. The focus will be on some key indicators like standard deviation, mean, C.V.%, $R^2$, adjusted $R^2$, predicted $R^2$, and acceptable levels of precision. Each of these indicators provides vital information regarding the strength and dependability of the quadratic model utilized in this investigation. The standard deviation (SD) of 0.3659 was the average difference between the observed and fitted values. A low standard deviation indicates a close alignment between the model predictions and the experimental data, demonstrating a high level of precision in the model. The low value of residuals indicates that there is minimal variation in the degradation efficiency of MB, which further confirms the accuracy of the model in capturing this variability [28].

The $R^2$ value of 0.9872 signifies that 98.72% of the variation in MB degrading efficiency can be accounted for by the model. The high $R^2$ value indicates the model's great ability to explain and capture the link between the inputs (starting pH, catalyst loading, and $H_2O_2$ dosage) and the response variable. The adjusted $R^2$ score of 0.9708, which considers the number of predictors in the model, is little lower but still indicates a strong level of fit. This indicates that the model maintains its strength even when accounting for the number of factors included, hence demonstrating its appropriateness for predicting the efficiency of MB deterioration.

https://doi.org/ 10.24191/esteem.v20iSeptember.1860.g1828

The forecasted $R^2$ value of 0.7957, although lower than the modified $R^2$, nevertheless suggests a satisfactory level of predictive precision. This metric quantifies the model's capacity to accurately forecast new observations, serving as an indicator of the model's ability to apply to unfamiliar data. While the predicted $R^2$ value is not as high as the $R^2$ and adjusted $R^2$ values, a value near to 0.8 indicates that the model is capable of accurately predicting the efficiency of MB deterioration under various experimental settings. However, there is still potential for enhancing the accuracy of these predictions [26].

Table 3. ANOVA results for the quadratic model

| Source | Sum of Squares | df | Mean Square | F-value | p-value | |
|---|---|---|---|---|---|---|
| **Model** | 72.46 | 9 | 8.05 | 60.14 | < 0.0001 | significant |
| A-initial pH | 37.32 | 1 | 37.32 | 278.76 | < 0.0001 | |
| B-Catalyst loading | 5.71 | 1 | 5.71 | 42.67 | 0.0003 | |
| C-$H_2O_2$ dosage | 4.86 | 1 | 4.86 | 36.31 | 0.0005 | |
| AB | 2.14 | 1 | 2.14 | 15.98 | 0.0052 | |
| AC | 0.0617 | 1 | 0.0617 | 0.4609 | 0.5190 | |
| BC | 0.0241 | 1 | 0.0241 | 0.1803 | 0.6839 | |
| $A^2$ | 13.91 | 1 | 13.91 | 103.86 | < 0.0001 | |
| $B^2$ | 2.77 | 1 | 2.77 | 20.65 | 0.0027 | |
| $C^2$ | 3.70 | 1 | 3.70 | 27.62 | 0.0012 | |
| **Residual** | 0.9372 | 7 | 0.1339 | | | |
| Lack of Fit | 0.9372 | 3 | 0.3124 | | | |
| Pure Error | 0.0000 | 4 | 0.0000 | | | |
| **Cor Total** | 73.40 | 16 | | | | |

Table 4. Regression analysis of the ANOVA

| Std. Dev. | Mean | C.V. % | $R^2$ | Adjusted $R^2$ | Predicted $R^2$ | Adeq Precision |
|---|---|---|---|---|---|---|
| 0.3659 | 95.73 | 0.3822 | 0.9872 | 0.9708 | 0.7957 | 24.6824 |

### 3.3 Response surface analysis

The three-dimensional surface and contour plots illustrate the relationship between the initial pH and catalyst loading at constant $H_2O_2$ dosages, as shown in Fig. 1(a) and Fig.1 b). It can be observed from these graphical representations that higher levels of both pH and catalyst loading increased MB decolorization. The pronounced curvature of the response surface indicated that both variables had significant effects. As pointed out by Song et al.[10], optimum decolorization was achieved with both high pH and catalyst dosage. Their findings showed that $Fe_3O_4$ nanoparticles became more effective for dye degradation at high pH values because of the better dispersion and stability of $Fe_3O_4$ NPs. Fig. 1(c) and Fig. 1(d) present the relationship between the initial pH value and $H_2O_2$ dosage while maintaining a constant catalyst dosage. The surface plot highlights that the efficiency of decolorization was significantly affected by both the pH level and dosage of $H_2O_2$. In essence, an increase in pH, combined with a moderate increase in $H_2O_2$ dosage, favors effectiveness. In addition, excess hydrogen peroxide ($H_2O_2$) has adverse effects on efficiency owing to its scavenging effects, according to Pignatello et al. [39]. The contour plot indicates that optimal

https://doi.org/ 10.24191/esteem.v20iSeptember.1860.g1828

decolorization is attained with a high pH value coupled with a moderate amount of $H_2O_2$, stressing the importance of sustaining an appropriate balance.

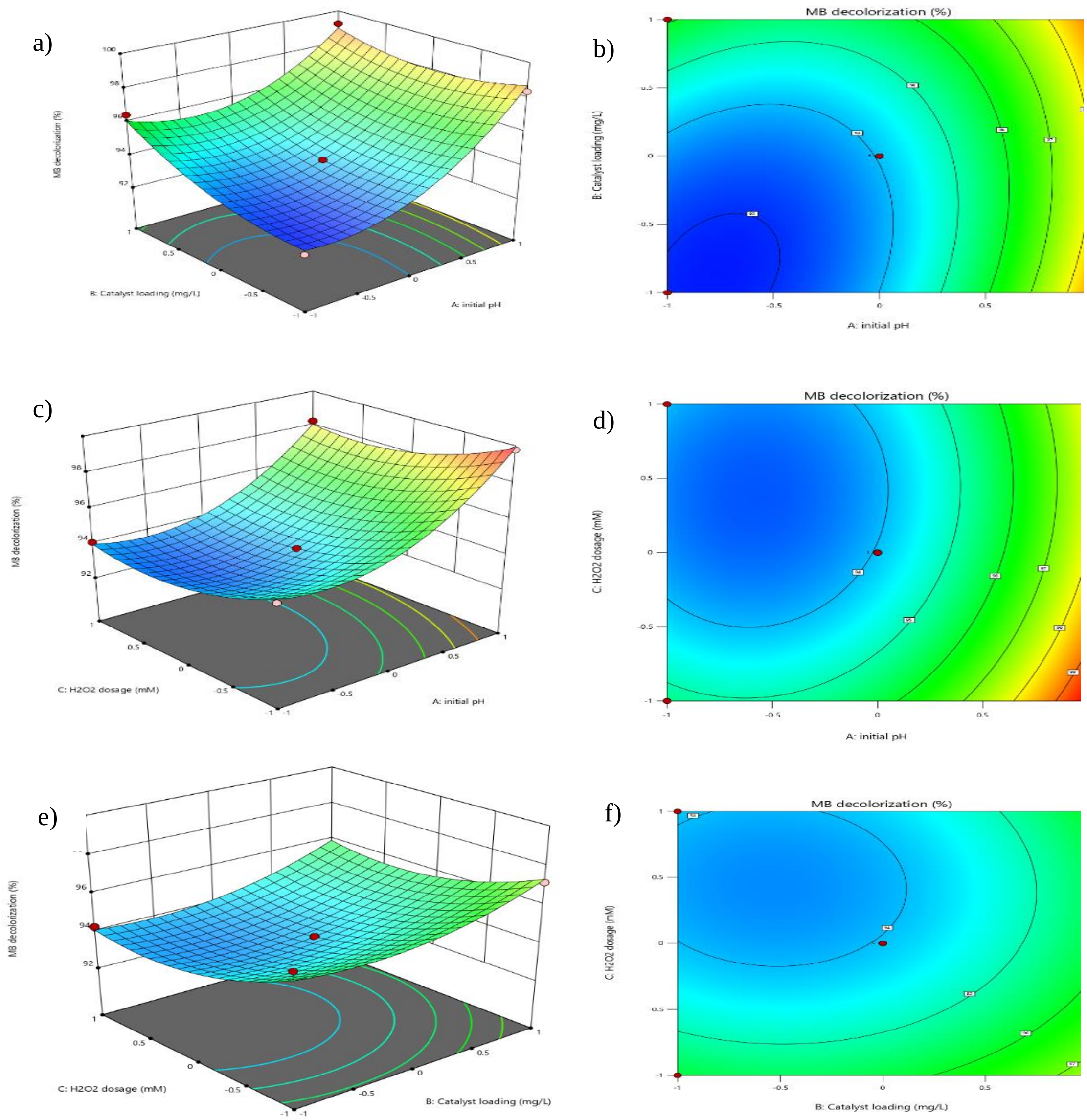


Fig. 1. Contour graphs of MB degradation highlighting (a) and (b) the relationship between the initial pH and catalyst loading with constant $H_2O_2$ dosage, (c) and (d) the relationship between the initial pH and $H_2O_2$ dosage with constant catalyst loading, and (e) and (f) the relationship between catalyst loading and $H_2O_2$ dosage with constant initial pH

Fig. 1(e) and Fig. 1(f) illustrate the correlation between the catalyst loading and $H_2O_2$ dosage while maintaining a constant starting pH. Both factors, therefore, favored efficiency in decolorization. Their interaction, however, indicates that at higher levels, benefits decrease. Maximum efficiency was achieved with an optimum dose of the catalyst and $H_2O_2$. The contour plot, as illustrated, highlights that peak

https://doi.org/ 10.24191/esteem.v20iSeptember.1860.g1828

efficiency is located at intermediate values that support a trade-off between catalytic activity and hydroxyl radicals' availability according to Gogate and Pandit [40]. The contour graphs give an in-depth overview of how to develop the Fenton-like reaction in the best way to degrade MB. Specifically, , the large effects of initial pH, catalyst loading, and dosage of $H_2O_2$ interact with each other. These results imply that an integrated approach must be developed in pursuit of optimal degradation efficiency, as further confirmed by regression analysis and ANOVA.

### 3.4 Model validation

Table 5 illustrated the validation experiments of optimized settings for MB degradation. The optimal settings obtained from the analyses of regression and ANOVA were used and the prediction accuracy and reliability of the developed model were further tested. The investigated parameters were initially fixed at an optimum value of pH = 7, catalyst dosage of 10 g/L, and $H_2O_2$ dose of 10 mM. These validation runs provided the expected values of the actual percentage of MB decolorization, under the experimental conditions, with a negligible percentage of error. For example, in Run 1, the actual decolorization efficiency was 99.89%, which was slightly lower than the projected efficiency of 99.94%, resulting in an extremely small error of 0.05%. The robust match between the experimental and anticipated values confirms the reliability of the quadratic model for properly forecasting the deterioration of the MB under optimized settings. The consistently low percentage errors (<5% mistakes) recorded in all validation trials indicate that the optimized conditions obtained from the model are both dependable and effective for degrading the MB. The reproducibility of the optimized settings is highlighted by the consistency in the testing results, which makes them well suited for practical applications in wastewater treatment. The results confirm that the model is effective in predicting the results of the Fenton-like reaction using $Fe_3O_4$ nanoparticles/PVDF macrospheres. This ensured that the reaction parameters could be precisely controlled, leading to a high degradation efficiency.

Table 5. Validation run of the optimized setting for the MB degradation process condition

| Run | Initial pH | Catalyst loading | $H_2O_2$ dosage | MB decolorization (%) – experimental | MB decolorization (%) – predicted | % error |
|---|---|---|---|---|---|---|
| 1 | 7 | 10 g/L | 10 mM | 99.89 | 99.94 | 0.05 |
| 2 | 7 | 10 g/L | 10 mM | 98.76 | 99.94 | 1.18 |
| 3 | 7 | 10 g/L | 10 mM | 98.55 | 99.94 | 1.39 |
| 4 | 7 | 10 g/L | 10 mM | 98.64 | 99.94 | 1.31 |
| 5 | 7 | 10 g/L | 10 mM | 99.23 | 99.94 | 0.71 |

## 4. CONCLUSION

The focus of the present study aimed to enhance the breakdown of methylene blue (MB) dye by utilizing a heterogeneous Fenton-like reaction involving $Fe_3O_4$ nanoparticle/PVDF macrospheres. By employing the Response Surface Methodology (RSM) and Box-Behnken design (BBD), the study determined the best circumstances for obtaining a degradation efficiency of 99.94%. These settings included a pH of 7, a catalyst concentration of 10 g/L, and $H_2O_2$ concentration of 10 mM. It can be observed from the output of regression analysis and ANOVA that the factors, in particular pH, played an influential role. The model was reliable enough as there is a fair relationship between the predicted and actual values. This approach ensures the rate and efficiency of the catalytic system toward large-scale treatment of wastewater, yielding good quality water with minimal contamination. The stability of the catalysts has to be ascertained by further studies, which also should also determine the order of degradation of other pollutants.

https://doi.org/ 10.24191/esteem.v20iSeptember.1860.g1828

## 5. ACKNOWLEDGEMENTS/FUNDING

This work was partly supported by the EMZI-UiTM Nanoparticle Colloids & Interface Industrial Research Laboratory under an industrial grant, MIH-(008/2020). We would also want to thank the Ministry of Higher Education, Malaysia, under Fundamental Research Grant Scheme with No. FRGS//1/2022/STG05/UITM/02/10), for the encouragement given to us during this study.

## 6. CONFLICT OF INTEREST STATEMENT

The authors agree that this research was conducted in the absence of any self-benefits or commercial or financial conflicts and declare the absence of conflicting interests with the funders.

## 7. AUTHORS' CONTRIBUTIONS

**Mohamed Syazwan Osman**: Conceptualization, Funding acquisition, methodology, formal analysis, investigation and writing-original draft; **Huzairy Hassan**: Supervision, Project administration, writing-review and editing, and validation; **Sung-Ting Sam**: Supervision, writing- review and editing, and validation; **Nadzirah Balqis Mohd Nazeri**: Methodology, formal analysis, investigation**. Mohd Syafiq Abdul Wahab**: Methodology, formal analysis, investigation. **Rasyidah Alrozi**: writing review, editing, and validation. **Hafawati Rosdi**: writing- review and editing, **Maya Fitriyanti**: writing- review and editing.

## 8. REFERENCES

[1] A. A. Bayode, F. O. Agunbiade, M. O. Omorogie, R. Moodley, O. Bodede, and E. I. Unuabonah, "Clean technology for synchronous sequestration of charged organic micro-pollutant onto microwave-assisted hybrid clay materials," *Environmental Science and Pollution Research*, vol. 27, no. 9, pp. 9957–9969, 2020. Available: doi: 10.1007/s11356-019-07563-z.

[2] H. Kolya and C. W. Kang, "Toxicity of Metal Oxides, Dyes, and Dissolved Organic Matter in Water: Implications for the Environment and Human Health," *Multidisciplinary Digital Publishing Institute (MDPI)*, vol. 12, no. 2, p. 111, 2021. Available: doi: 10.3390/toxics12020111.

[3] P. O. Oladoye, T. O. Ajiboye, E. O. Omotola, and O. J. Oyewola, "Methylene blue dye: Toxicity and potential elimination technology from wastewater," *Elsevier B.V.*, vol. 16, p. 100678, 2021. Available: doi: 10.1016/j.rineng.2022.100678.

[4] R. Alrozi, N. A. Zamanhuri, and M. S. Osman, "Removal of methylene blue from aqueous solution by adsorption onto NaOH-treated rambutan peel," in *BEIAC 2012 - 2012 IEEE Business, Engineering and Industrial Applications Colloquium*, pp. 92–97, 2012. Available: doi: 10.1109/BEIAC.2012.6226113.

[5] N. Amri, R. Alrozi, M. S. Osman, N. Nasuha, and N. S. Aman, "Removal of methylene blue dye from aqueous solution using pink guava (Psidium Guajava) waste-based activated carbon," in *SHUSER 2012 - 2012 IEEE Symposium on Humanities, Science and Engineering Research*, pp. 33–38, 2012. Available: doi: 10.1109/SHUSER.2012.6268867.

[6] J. Lin *et al.*, "Environmental impacts and remediation of dye-containing wastewater," *Nat Rev Earth Environ*, vol. 4, no. 11, pp. 785–803, 2023. Available: doi: 10.1038/s43017-023-00489-8.

[7] M. Rafatullah, O. Sulaiman, R. Hashim, and A. Ahmad, "Adsorption of methylene blue on low-cost adsorbents: A review," *J Hazard Mater*, vol. 177, no. 1–3, pp. 70–80, 2010. Available: doi: 10.1016/j.jhazmat.2009.12.047.

[8] S. Mohammadpour, P. N. Moghadam, and P. Gharbani, "Preparation, characterization, and photocatalytic performance of a PVDF/cellulose membrane modified with nano Fe3O4 for

https://doi.org/ 10.24191/esteem.v20iSeptember.1860.g1828

removal of methylene blue using RSM under visible light," *RSC Adv*, vol. 14, no. 13, pp. 8801–8809, 2024. Available: doi: 10.1039/d3ra08599f.

[9] N. Isa, M. S. Osman, H. Abdul Hamid, V. Inderan, and Z. Lockman, "Studies of surface plasmon resonance of silver nanoparticles reduced by aqueous extract of shortleaf spikesedge and their catalytic activity," *Int J Phytoremediation*, vol. 25, no. 5, pp. 658–669, 2023. Available: doi: 10.1080/15226514.2022.2099345.

[10] S. Song *et al.*, "Ultrasmall Graphene Oxide Modified with Fe3O4 Nanoparticles as a Fenton-Like Agent for Methylene Blue Degradation," *ACS Appl Nano Mater*, vol. 2, no. 11, pp. 7074–7084, 2019. Available: doi: 10.1021/acsanm.9b01608.

[11] Y. J. Zhang, J. J. Chen, G. X. Huang, W. W. Li, H. Q. Yu, and M. Elimelech, "Distinguishing homogeneous advanced oxidation processes in bulk water from heterogeneous surface reactions in organic oxidation," *Proc Natl Acad Sci U S A*, vol. 120, no. 20, 2023. Available: doi: 10.1073/pnas.2302407120.

[12] N. A. Zubir, C. Yacou, X. Zhang, and J. C. Diniz Da Costa, "Optimisation of graphene oxide-iron oxide nanocomposite in heterogeneous Fenton-like oxidation of Acid Orange 7," *J Environ Chem Eng*, vol. 2, no. 3, pp. 1881–1888, 2014. Available: doi: 10.1016/j.jece.2014.08.001.

[13] M. G. Tavares *et al.*, "Reusable iron magnetic catalyst for organic pollutant removal by Adsorption, Fenton and Photo Fenton process," *J Photochem Photobiol A Chem*, vol. 432, Nov. 2022. Available: doi: 10.1016/j.jphotochem.2022.114089.

[14] S. P. Yeap, J. K. Lim, B. S. Ooi, and A. L. Ahmad, "Agglomeration, colloidal stability, and magnetic separation of magnetic nanoparticles: collective influences on environmental engineering applications," *Journal of Nanoparticle Research*, vol. 19, no. 11, 2017. Available: doi: 10.1007/s11051-017-4065-6.

[15] S. P. Yeap, A. L. Ahmad, B. S. Ooi, and J. Lim, "Electrosteric stabilization and its role in cooperative magnetophoresis of colloidal magnetic nanoparticles," *Langmuir*, vol. 28, no. 42, pp. 14878–14891, 2012. Available: doi: 10.1021/la303169g.

[16] J. Lim, S. P. Yeap, and S. C. Low, "Challenges associated to magnetic separation of nanomaterials at low field gradient," *Sep Purif Technol*, vol. 123, pp. 171–174, 2014. Available: doi: 10.1016/j.seppur.2013.12.038.

[17] L. P. Kong *et al.*, "Design and synthesis of magnetic nanoparticles augmented microcapsule with catalytic and magnetic bifunctionalities for dye removal," *Chemical Engineering Journal*, vol. 197, pp. 350–358, 2012. Available: doi: 10.1016/j.cej.2012.05.019.

[18] M. S. Osman, L. P. Kong, N. A. Zamanhuri, and J. K. Lim, "Role of Temperature and pH on the Dye Degradation Using Magnetic Nanoparticles Augmented Polymeric Microcapsule," *Adv Mat Res*, vol. 1113, pp. 566–570, 2015. Available: doi: 10.4028/www.scientific.net/amr.1113.566.

[19] M. S. Osman *et al.*, "Artificial Neural Network-driven Optimization of Fe3O4 Nanoparticles/PVDF Macrospheres in Fenton-like System for Methylene Blue Degradation," *Journal of Advanced Research in Micro and Nano Engineering*, vol. 22, no. 1, pp. 68–84, 2024. Available: https://doi.org/10.37934/armne.22.1.6884.

[20] S. Y. Wai, S. P. Yeap, and Z. A. Jawad, "Synthesis of magnetite macro-bead for water remediation: Process optimization via manipulation of bead size and surface morphology," in *IOP Conference Series: Earth and Environmental Science*, 2020. Available: doi: 10.1088/1755-1315/463/1/012177.

[21] A. Shokri and M. S. Fard, "A critical review in Fenton-like approach for the removal of pollutants in the aqueous environment," *Elsevier B.V.*, vol. 7, p. 100534, 2022. Available: doi: 10.1016/j.envc.2022.100534.

[22] I. Afzal *et al.*, "Logical Optimization of Metal-Organic Frameworks for Photocatalytic Degradation of Organic Pollutants in Water via Box-Behnken Design," *ACS ES and T Water*, vol. 2, no. 2, pp. 648–660, 2023. Available: doi: 10.1021/acsestwater.3c00667.

https://doi.org/ 10.24191/esteem.v20iSeptember.1860.g1828

[23] H. M. Nassef, G. A. A. M. Al-Hazmi, A. A. A. Alayyafi, M. G. El-Desouky, and A. A. El-Bindary, “Synthesis and characterization of new composite sponge combining of metal-organic framework and chitosan for the elimination of Pb(II), Cu(II) and Cd(II) ions from aqueous solutions: Batch adsorption and optimization using Box-Behnken design,” *J Mol Liq*, vol. 394, 2024. Available: doi: 10.1016/j.molliq.2023.123741.

[24] K. G. N. Quiton, Y. H. Huang, and M. C. Lu, “Photocatalytic oxidation of Reactive Red 195 by bimetallic Fe–Co catalyst: Statistical modeling and optimization via Box-Behnken design,” *Chemosphere*, vol. 338, 2023. Available: doi: 10.1016/j.chemosphere.2023.139509.

[25] M. A. M. Ariff, S. Tukiman, N. A. A. Razak, M. S. Osman, and J. Jaapar, “Optimization of supercritical fluid extraction of Mariposa Christia Vespertilionis leaves towards antioxidant using response surface methodology,” in *Journal of Physics: Conference Series*, 2019. Available: doi: 10.1088/1742-6596/1349/1/012054.

[26] M. Alishiri, S. A. Abdollahi, A. N. Neysari, S. F. Ranjbar, N. Abdoli, and M. Afsharjahanshahi, “Removal of ciprofloxacin and cephalexin antibiotics in water environment by magnetic graphene oxide nanocomposites; optimization using response surface methodology,” *Results in Engineering*, vol. 20, 2023. Available: doi: 10.1016/j.rineng.2023.101507.

[27] K. Khairudin, N. F. Abu Bakar, and M. S. Osman, “Magnetically recyclable flake-like BiOI-Fe3O4 microswimmers for fast and efficient degradation of microplastics,” *J Environ Chem Eng*, vol. 10, no. 5, p. 108275, 2022. Available: doi: https://doi.org/10.1016/j.jece.2022.108275.

[28] R. R. Kalantary, M. Farzadkia, M. Kermani, and M. Rahmatinia, “Heterogeneous electro-Fenton process by Nano-Fe3O4 for catalytic degradation of amoxicillin: Process optimization using response surface methodology,” *J Environ Chem Eng*, vol. 6, no. 4, pp. 4644–4652, 2018. Available: doi: 10.1016/j.jece.2018.06.043.

[29] N. Kanmaz and M. Buğdaycı, “Promoting photo-fenton catalytic performance of novel NiZrO3-type perovskite: Optimization with response surface methodology,” *J Mol Struct*, vol. 1295, 2024. Available: doi: 10.1016/j.molstruc.2023.136718.

[30] F. Jackulin, P. Senthil Kumar, and G. Rangasamy, “Degradation of tartrazine dye using advanced oxidation process: Application of response surface methodology for optimization,” *Desalination Water Treat*, vol. 317, p. 100066, 2024. Available: doi: 10.1016/j.dwt.2024.100066.

[31] Y. Liu, Y. Zhao, and J. Wang, “Fenton/Fenton-like processes with in-situ production of hydrogen peroxide/hydroxyl radical for degradation of emerging contaminants: Advances and prospects,” *Elsevier B.V.*, vol. 404, p. 124191, 2021. Available: doi: 10.1016/j.jhazmat.2020.124191.

[32] N. Wang, T. Zheng, G. Zhang, and P. Wang, “A review on Fenton-like processes for organic wastewater treatment,” *Elsevier Ltd*., vol. 4, no. 1, pp. 762-787, 2016. Available: doi: 10.1016/j.jece.2015.12.016.

[33] D. Meyerstein, “Re-examining Fenton and Fenton-like reactions,” *Nature Research*, vol. 5, pp. 595–597, 2021. Available: doi: 10.1038/s41570-021-00310-4.

[34] Y. Jiang *et al.*, “Recent progress in Fenton/Fenton-like reactions for the removal of antibiotics in aqueous environments,” *Academic Press*, vol. 236, p. 113464, 2022. Available: doi: 10.1016/j.ecoenv.2022.113464.

[35] Q. Zhang, X. Yang, and J. Guan, “Applications of Magnetic Nanomaterials in Heterogeneous Catalysis,” *ACS Appl Nano Mater*, vol. 2, no. 8, pp. 4681–4697, 2019. Available: doi: 10.1021/acsanm.9b00976.

[36] J. Wang and J. Tang, “Fe-based Fenton-like catalysts for water treatment: Catalytic mechanisms and applications,” *Elsevier B.V*, vol. 332, p. 115755, 2021. Available: doi: 10.1016/j.molliq.2021.115755.

[37] I. Amalraj Appavoo, J. Hu, Y. Huang, S. F. Y. Li, and S. L. Ong, “Response surface modeling of Carbamazepine (CBZ) removal by Graphene-P25 nanocomposites/UVA process using central composite design,” *Water Res*, vol. 57, pp. 270–279, 2014. Available: doi: 10.1016/j.watres.2014.03.007.

https://doi.org/ 10.24191/esteem.v20iSeptember.1860.g1828

[38] N. Thomas, D. D. Dionysiou, and S. C. Pillai, "Heterogeneous Fenton catalysts: A review of recent advances," *Elsevier B.V.,* vol. 404, p. 124082, 2021. Available: doi: 10.1016/j.jhazmat.2020.124082.

[39] J. J. Pignatello, E. Oliveros, and A. MacKay, "Advanced oxidation processes for organic contaminant destruction based on the fenton reaction and related chemistry," *Critical Reviews in Environmental Science and Technology*, vol. 36, no. 1, pp. 1–84, 2006. Available: doi: 10.1080/10643380500326564.

[40] P. R. Gogate and A. B. Pandit, "A review of imperative technologies for wastewater treatment I: Oxidation technologies at ambient conditions," *Advances in Environmental Research*, vol. 8, no. 3–4, pp. 501–551, 2004. Available: doi: 10.1016/S1093-0191(03)00032-7.



https://doi.org/ 10.24191/esteem.v20iSeptember.1860.g1828